Phase-locked laser diode interferometer: high-speed feedback control system

Takamasa Suzuki, Osmai Sasaki, Katsuhiro Higuchi, and Takeo Maruyama

We have previously proposed a phase-locked laser diode interferometer. In that previous interferometer, however, there was substantial room for improvement in the reduction of measurement time. This reduction is achieved by using a different process for generation of the feedback signal in which the output of a charge-coupled device image sensor is used effectively. We analyze the feedback control system of the interferometer as a discrete-time system and discuss the characteristics of the interferometer. It is shown that the measurement time is much shorter than that of the interferometer proposed previously.

I. Introduction

Recently, a laser diode (LD) was used as a light source in heterodyne interferometers. The phase modulation required by the interferometers is easily produced by modulating the injection current of the LD, thus changing the wavelength in the LD. By effective use of this aspect of the LD, we can construct a phase-locked laser diode (PLLD) interferometer[1] without the mechanical elements that were used in the conventional phase-locked interferometers.[2–4] The PLLD interferometer detects information about phase α in the interference signal with sinusoidal phase-modulating interferometry.[5–7] Scanning a measuring point along the surface of the object, the phase changes according to the surface profile of the object. This phase displacement is stabilized by controlling the injection current of the LD. The surface profile is obtained from the amount of change in the injection current.

The PLLD interferometer does not need a computer for computation. It uses a feedback control system to obtain the surface profile. Thus, the construction of the PLLD interferometer is simple, and it enables one to measure the surface profile in real time. The measurement time depends on the response time of the feedback control system. Consequently, how the feedback control signal is generated and how the injection current is controlled are important.

The authors are with the Faculty of Engineering, Niigata University, 8050 Ikarashi 2, Niigata-shi 950-21, Japan.

Received 20 March 1990.
0003-6935/91/253622-05$05.00/0.

In surface profile measurement, a charge-coupled device (CCD) image sensor is often used to detect the distribution of interference signals. In Ref. 1, the CCD image sensor integrates the sinusoidal phase-modulated interference signal for each period of the charge storage at each measurment point. The interference signal is detected as a discrete signal in time. This signal is multiplied by a sinusoidal wave signal, which is used for the sinusoidal phase modulation, and is low pass filtered to obtain a continuous feedback signal sin α in time. The low-pass filter limits the response time of the feedback system. In Ref. 1, the frequency of the phase modulation is 1.8 kHz, and the cutoff frequency of the low-pass filter is 100 Hz. The shortest response time or scanning time is ~80 ms.

We constructed a PLLD interferometer that measures surface profiles more rapidly than that in Ref. 1. The feedback signal is generated directly from the output of the CCD image sensor without using a low-pass filter. The period of charge storage in the CCD image sensor is set to one half of the period of the sinusoidal phase modulation. The output of the CCD image sensor is obtained once each charge storage period, so that the feedback control system is a time-discrete system. We analyzed this system with a z transform to construct an optimum proportional-integral (PI) controller. It is shown that the measurement time of the PLLD interferometer reported here is greatly reduced when compared with a PLLD interferometer using a low-pass filter.

II. Principle

Figure 1 shows the setup of the PLLD interferometer whose optical system is the same as that reported in Ref. 1. Sinuosidal phase modulation is obtained using the modulation current

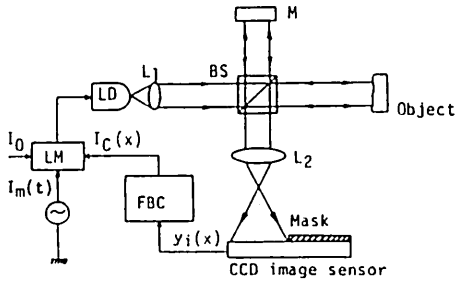

Fig. 1. Experimental setup of the PLLD interferometer.

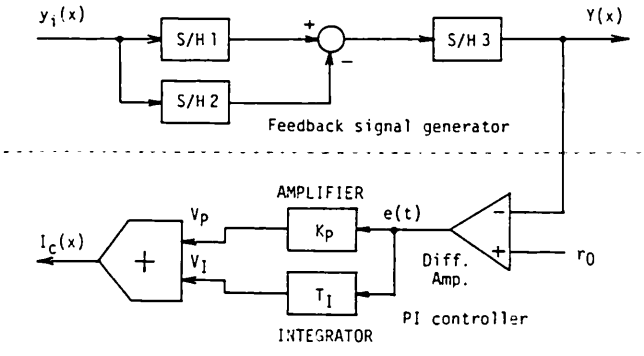

Fig. 2. Block diagram of the FBC.

$$I_m(t) = a \cos \omega_c t. \tag{1}$$

The surface of the object is represented by $D(x)$, where x is the measurement position on the surface of the object. The optical path difference between the two arms is $2D_0$ at position x_0, where $D(x_0)$ is regarded as zero. The central wavelength λ_0 of the LD is determined by its dc bias current I_0. The wavelength $\lambda_c(x)$ changes with the feedback control of the injection current $I_c(x)$ according to the relationship $\lambda_c(x) = \beta I_c(x)$, where β is the modulation efficiency of the LD. The interference signal on the CCD image sensor is

$$S(t, x) = S_1 + S_0 \cos[z \cos \omega_c t + \alpha(x)], \tag{2}$$

where

$$z = (4\pi/\lambda_0^2)a\beta D_0,$$

$$\alpha(x) = [4\pi/[\lambda_0 + \lambda_c(x)]][D_0 + D(x)], \tag{3}$$

and S_1 is a dc component. When we scan the measuring point along the surface of the object, the phase $\alpha(x)$ changes according to the surface profile if the current $I_c(x)$ is fixed. The current $I_c(x)$ must be controlled if the phase $\alpha(x)$ is to be locked to a specified value $\alpha(x_0)$. The surface profile of the object $D(x)$ from the control current $I_c(x)$ is obtained as follows:

$$D(x) = (D_0/\lambda_0)\beta I_c(x), \tag{4}$$

where $I_c(x_0) = 0$.

Phase locking is achieved by controlling the injection current $I_c(x)$ with a feedbck system. A block diagram of the feedback controller (FBC) is shown in Fig. 2. Although the quantities in Fig. 2 are functions of both the measuring point x and time t, we present them in forms of only one of the two variables to obtain a clear description of the FBC. The feedback signal

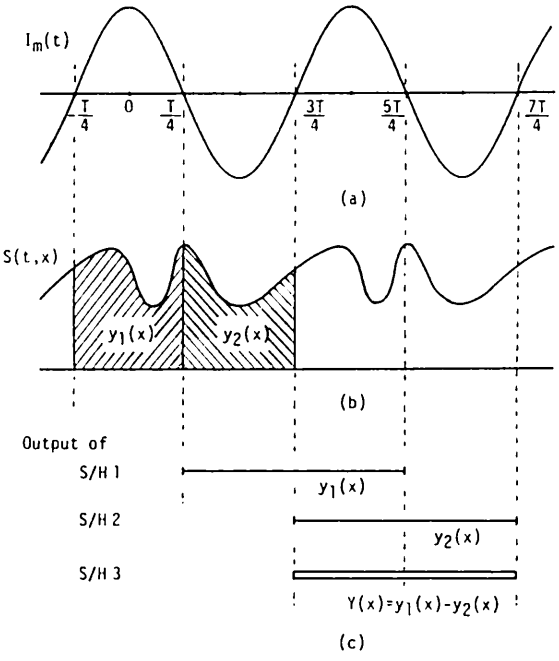

Fig. 3. Generation of the feedback signal: (a) modulation current, (b) interference signal $S(t, x)$, and (c) output signals of the sample-hold circuits.

$Y(x)$ is generated from the output signals $y_i(x)$ of the CCD image sensor, and the control current $I_c(x)$ is generated from the feedbck signal $Y(x)$ using a PI controller. In Sections III and IV, we explain the FBC in detail.

III. Generation of the Feedback Signal

The schematic explanation of the generation of the feedback signal is shown in Fig. 3. Figures 3(a) and 3(b) show the modulation current $I_m(t)$ and the interference signal $S(t, x)$, respectively. The CCD image sensor is driven synchronously with the modulation current $I_m(t)$. The signal $S(t, x)$ is integrated during a half-period of the modulation current $I_m(t)$. The CCD image sensor produces the signals[7]

$$y_i(x) \int_{(T/4)(2i-3)}^{(T/4)(2i-1)} S(t, x)\mathrm{d}t$$

$$= (T/2)[S_1 + J_0(z)S_0 \cos \alpha(x) + h_i S_0 \sin \alpha(x)], \tag{5}$$

where

$$h_{2m} = -h_{2m-1} = -(4/\pi) \sum_{n=1}^{\infty} [J_{2n-1}(z)/2n - 1],$$

$T = 2\pi/\omega_c$, $J_n(z)$ is the nth-order Bessel function, and i and m are the integers.

We restrict our attention to the one period between $-T/4$ and $3T/4$ corresponding to the timing at $i = 1$ and $i = 2$. The CCD image sensor outputs the signals $y_1(x)$ and $y_2(x)$ at times $T/4$ and $3T/4$, respectively, as shown in Fig. 3(b). A sample-hold circuit 1 (S/H1) holds the signal $y_1(x)$ during the period T, and S/H2 holds the signal $y_2(x)$ during the same period that is shown in Fig. 3(c). By subtracting $y_2(x)$ from $y_1(x)$, we obtain the feedback signal:

$$Y(x) = y_1(x) - y_2(x)$$
$$= K_1 \sin \alpha(x), \quad (6)$$

where $K_1 = S_0 h_2 T$. S/H3 holds the signal $Y(x)$ between $3T/4$ and $7T/4$. This processing is done for every interval T. Thus the signal $Y(x)$ is discrete in time.

IV. Feedback Control System

We describe the feedback control system that uses the PI controller to eliminate the steady-state error. As shown in Fig. 2, a differential amplifier whose gain is K_d produces an error signal $e(t)$, which is the difference between the feedback signal $Y(x)$ and a reference signal r_0. The object phase or the locked phase is determined by the reference signal r_0. The error signal $e(t)$ is fed to an amplifier with gain K_P and to an integrator with time constant T_I. The proportional output V_P and the integral output V_I are added, and the voltage output is converted to a control current $I_c(x)$.

The system is analyzed as a discrete-time control system, since the feedback signal is obtained at discrete intervals T. A block diagram of the feedback control system is shown in Fig. 4, where variable s represents a Laplace operation. The transfer function $G_h(s)$ represents a hold circuit that holds the sampled error signal $e(kT)$ during the period T, and it is given by

$$G_h(s) = [1 - \exp(-Ts)]/s, \quad (7)$$

where k is the sampling number. The transfer function of the PI controller is given by

$$G_c(s) = K_d[K_P + (1/T_I s)]. \quad (8)$$

The control current $I_c(x)$ changes the phase of the interference signal by $\lambda_c(x)$, which is represented by the transfer function

$$G_a(s) = 4\pi\beta D_0/\lambda_0^2. \quad (9)$$

The product of the transfer functions $G_c(s)$ and $G_a(s)$ is denoted by the transfer function $G_t(s)$. The transfer function $G_d(s) = 4\pi/\lambda_0$ converts the displacement $D(x)$, which is caused by scanning a measuring point along the surface of the object, to the disturbed phase $\alpha_d(x)$. The sum of $\alpha_c(x)$ and $\alpha_d(x)$ is $\alpha(x)$. Since $\alpha(x)$ is always controlled to be approximately an integer multiple of 2π, $\sin \alpha(x)$ can be approximated as $\alpha(x)$. Then the transfer function $G_s(s)$ becomes K_1 as given in Eq. (6).

The z transform of the error $e(kT)$ caused by the displacement $D(x)$ is given by

$$E(z) = -\mathcal{Z}\{G_d(s)G_s(s)D(s)\}/[1 + \mathcal{Z}\{G_c(s)G_h(s)G_t(s)\}], \quad (10)$$

where $\mathcal{Z}\{f(s)\}$ denotes the z transform of $f(s)$. When the displacement $D(x)$ is a step whose amplitude is d, Eq. (10) is written as

$$E(z) = -[K_1 K_3/(1 + K_1 K_2 K_P)]d \times z/[z - \{1 - K_1 K_2 T/(1 + K_1 K_2 K_P)T_I\}], \quad (11)$$

where $K_d G_a(s)$ and $G_d(s)$ are replaced by K_2 and K_3, respectively. By taking the inverse z transform of $E(z)$, the error $e(kT)$ is obtained:

$$e(kT) = -[1 - \{K_1 K_2 T/(1 + K_1 K_2 K_P)T_I\}]^k \times [K_1 K_3/(1 + K_1 K_2 K_P)]d. \quad (12)$$

If the control parameters satisfy the condition

$$0 < K_1 K_2 T/(1 + K_1 K_2 K_P)T_I < 1, \quad (13)$$

phase locking is achieved because the error $e(kT)$ approaches zero according to the increase in k. Moreover, Eq. (12) indicates that the time required to achieve phase locking (i.e., the settling time) becomes shorter as $K_1 K_2 T/[(1 + K_1 K_2 K_P)T_I]$ approaches unity. If the control parameters are selected so that

$$K_1 K_2 K_P > 1, \quad (14)$$

Eq. (12) is approximated:

$$e(kT) = -(K_3/K_2 K_P)d[1 - T/K_P T_I]^k. \quad (15)$$

The settling time for phase locking depends largely on the sampling time T and the ratio $T/K_P T_I$. If the control parameters are selected to satisfy the condition in inequality (14), the influence of the gain K_1 or the reflection ratio is negligible.

V. Experiments

A. Experimental Setup

The experimental setup is shown in Fig. 1. We used a GaAlAs laser diode as the light source. Its maximum output power was 5 mW, and the central operating wavelength λ_0 was ~790 nm. The modulation efficiency β was 6×10^{-3} nm/mA. The optical path difference $2D_0$ was 140 mm. The frequency of phase modulation $1/T$ was 4 kHz. The pixel size of the CCD image sensor was 9×14 μm, and the pixels were arranged at

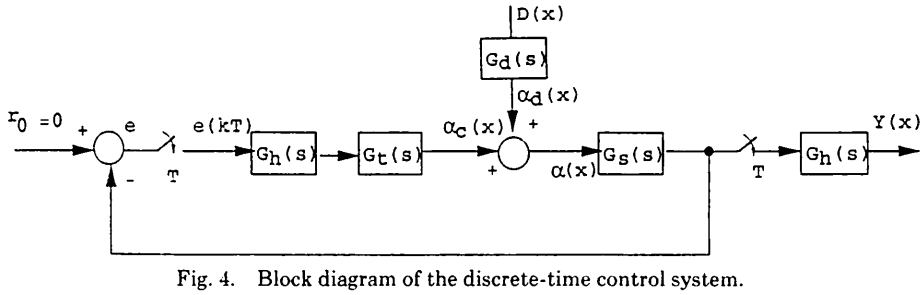

Fig. 4. Block diagram of the discrete-time control system.

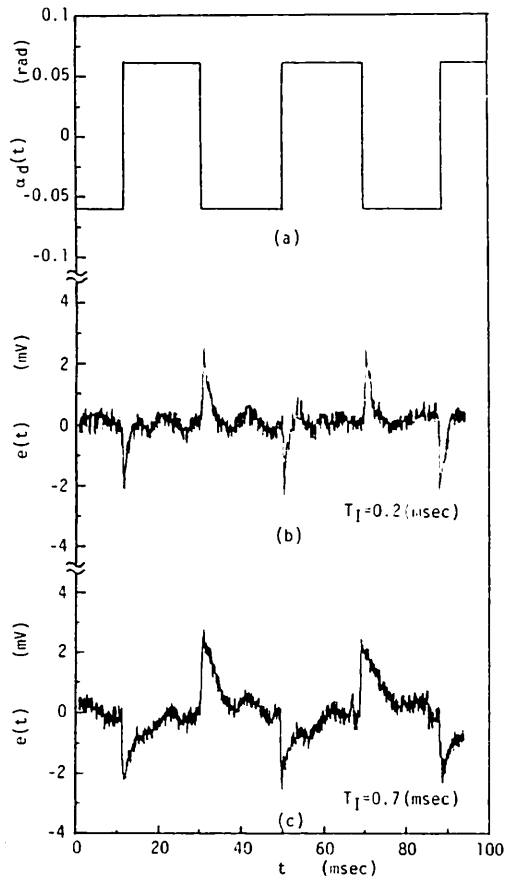

Fig. 5. Response of the error signal: (a) phase change caused by the piezoelectric transducer; (b), (c) error signals.

intervals of 14 μm. Fifty elements of the CCD image sensor were used to detect the interference signal; thus the number of measuring points was 50. The remaining elements were covered with black paper to eliminate unused light. The image of the surface of the object was formed on the CCD image sensor with a magnification of 3.0; thus the spatial interval of the measuring points was ~4.7 μm.

B. Settling Time

We discuss the theoretical results obtained from Eq. (12) by observing the error signal $e(t)$ experimentally. In this experiment, a mirror mounted on a piezoelectric transducer was used as an object, and we vibrated it with the rectangular signal shown in Fig. 5(a) instead of scanning the measuring point on the surface of the object. We could examine the settling time in the conditions of a constant reflection ratio of the object by using the vibrating mirror. The amount of phase change produced by the vibration of the mirror was ~0.06 rad. We obtained the value of the gain K_1 by measuring the amplitude of $Y(x)$. The gain K_1 was 400 mV/rad and was constant for the measuring points on the mirror. In the following experiments, the gains K_d and K_P were selected to be 0.07 and 2.0, respectively, to satisfy inequality (13) and to maintain stability in the control system. We judged that phase locking was achieved when the error signal $e(t)$ became smaller

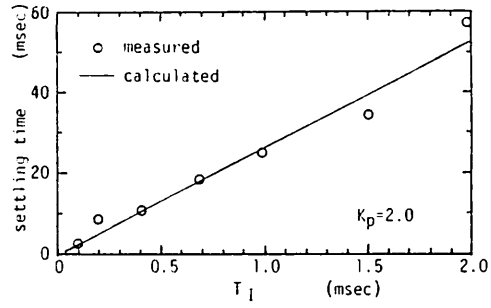

Fig. 6. Settling time as a function of integral time T_I.

than one-twentieth of its maximum value. We observed the error signals for the two different integral times as shown in Figs. 5(b) and 5(c). When T_I = 0.2 ms, the settling time was ~5 ms as shown in Fig. 5(b). Then the sampling number k was 20. When T_I = 0.7 ms, $e(t)$ had a significant value after 5 ms as shown in Fig. 5(c).

Next we measured the settling times for various integrating times. The measured settling times are shown in Fig. 6 as circular points. The theoretical settling times, which are calculated from Eq. (12), are shown in Fig. 6 by a solid line. The experimental results agree well with the theoretical curve. The results indicate that the feedback control system model shown in Fig. 4 is a reasonable approximation of the actual system. When we selected T_I = 0.1 ms with K_P = 2.0 and T = 0.25 ms, we obtained the shortest settling time of 2 ms in conditions where the system remains stable. In this case, the sampling number k is only 8. The settling time is short enough that real-time surface profile measurements can be realized with the PLLD interferometer.

C. Measurements of the Surface Profiles

We measured the surface profile of a diamond turned aluminum disk whose cutting pitch was ~50 μm.

First, we measured the surface profile of the disk with a Talystep instrument as shown in Fig. 7(a). The measurement interval was ~0.73 μm. The surface profile of the disk had a periodic structure determined by the cutting pitch, and the magnitude of the surface roughness of the disk was ~100 nm.

Next, we measured the surface profile of the same disk with the PLLD interferometer. According to the results in Subsection V.B, the proportional gain K_P and the integral time T_I were set to be 2.0 and 0.1 ms, respectively, to measure the surface profile as rapidly as possible. Although the settling time was expected to be ~2 ms with these values of the control variables, the scanning time T_{scan} was selected to be 8 ms to observe the error signal for a time period that is long compared with the settling time. T_{scan} is the time it takes to measure one point of the surface of the object. The measured surface profile is shown in Fig. 7(b). Since we measured 50 points at intervals of ~4.7 μm, it took 400 ms to measure the surface profile of the disk. The measuring points and their intervals in Fig. 7(a) are different from those in Fig. 7(b); thus the shapes of

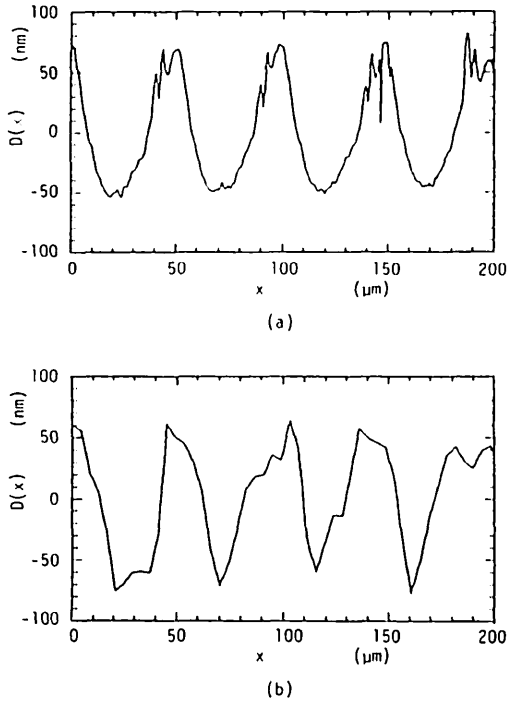

Fig. 7. Surface profiles measured with (a) the Talystep instrument and (b) the PLLD interferometer.

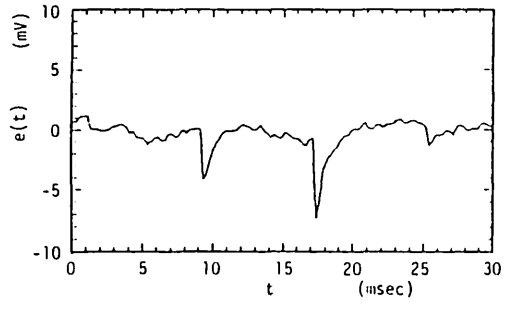

Fig. 8. Error signal $e(t)$ observed with the measurement of Fig. 7(b).

the profiles are somewhat different. But the peak-to-peak roughness and the period agree well, and the repeated measurement accuracy is estimated to be ~10 nm through a comparison of several measurements at the same position. We observed the error signal $e(t)$ at the same time, which is shown in Fig. 8. It indicates that phase locking is achieved so that the error signal $e(t)$ is substantially zero within the scanning time T_{scan}. Since the reflection ratio of the object was not constant, the gain K_1 varied at each measuring point. If the condition in inequality (14) is satisfied, phase lock is achieved in spite of variations in the gain K_1. The settling time is somewhat longer than 2 ms at some measuring points.

VI. Conclusions

It has been shown that a surface profile can be measured in a short time period by the PLLD interferometer proposed here. The settling time in the PLLD interferometer can be substantially decreased compared with when the PLLD interferometer utilizes a low-pass filter. We analyzed the feedback control system as a discrete-time system using the z transform. It has been shown that PLLD interferometry can be used to perform a profile measurement in real time. The influence of the reflection ratio on the surface of the object is nearly eliminated by the appropriate selection of control parameters. It seems that the measurement accuracy is below ~10 nm in this interferometer.

References

1. T. Suzuki, O. Sasaki, and T. Maruyama, "Phase locked laser diode interferometry for surface profile measurement," Appl. Opt. 28, 4407–4410 (1989).
2. D. T. Moore, R. Murray, and F. B. Neves, "Large aperture ac interferometer for optical testing," Appl. Opt. 17, 3959–3963 (1978).
3. G. W. Johnson, D. C. Leiner, and D. T. Moore, "Phase-locked interferometry," Opt. Eng. 18, 46–52 (1979).
4. H. J. Matthews, D. K. Hamilton, and C. J. R. Sheppard, "Surface profiling by phase-locked interferometry," Appl. Opt. 25, 2372–2374 (1986).
5. O. Sasaki and H. Okazaki, "Sinusoidal phase modulating interferometry for surface profile measurement," Appl. Opt. 25, 3137–3140 (1986).
6. O. Sasaki and H. Okazaki, "Analysis of measurement accuracy in sinusoidal phase modulating interferometry," Appl. Opt. 25, 3152–3158 (1986).
7. O. Sasaki, H. Okazaki, and M. Sakai, "Sinusoidal phase modulating interferometer using the integrating-bucket method," Appl. Opt. 26, 1089–1093 (1987).